

## Article

# Improving the Estimation of the Occurrence Time of an Impending Major Earthquake Using the Entropy Change of Seismicity in Natural Time Analysis

Panayiotis A. Varotsos<sup>1,2,\*</sup>, Nicholas V. Sarlis<sup>1,2</sup>, Efthimios S. Skordas<sup>1,2</sup>, Toshiyasu Nagao<sup>3</sup>, Masashi Kamogawa<sup>3</sup>, E. Leticia Flores-Márquez<sup>4</sup>, Alejandro Ramírez-Rojas<sup>5</sup> and Jennifer Perez-Oregon<sup>6</sup>

- <sup>1</sup> Section of Condensed Matter Physics, Department of Physics, National and Kapodistrian University of Athens, Panepistimiopolis, Zografos, 157 84 Athens, Greece; nsarlis@phys.uoa.gr (N.V.S.); eskordas@phys.uoa.gr (E.S.S.)
  - <sup>2</sup> Solid Earth Physics Institute, Department of Physics, National and Kapodistrian University of Athens, Panepistimiopolis, Zografos, 157 84 Athens, Greece
  - <sup>3</sup> Natural Disaster Research Section (NaDiR), Global Center for Asian and Regional Research, University of Shizuoka, 3-6-1, Takajo, Aoi-Ku, Shizuoka 420-0839, Japan; nagao@scc.u-tokai.ac.jp (T.N.); kamogawa@u-shizuoka-ken.ac.jp (M.K.)
  - <sup>4</sup> Instituto de Geofísica, Universidad Nacional Autónoma de México, Circuito Institutos S/N, Mexico City 04510, Mexico; leticia@igeofisica.unam.mx
  - <sup>5</sup> Departamento de Ciencias Básicas, Universidad Autónoma Metropolitana, Mexico City 14387, Mexico; alexramro@gmail.com
  - <sup>6</sup> Science and Engineering Department, Instituto Tecnológico y de Estudios Superiores de Monterrey, Ciudad López Mateos 52926, Mexico; jnnfr.po@gmail.com
- \* Correspondence: pvaro@otenet.gr; Tel.: +30-210-727-6737



**Citation:** Varotsos, P.A.; Sarlis, N.V.; Skordas, E.S.; Nagao, T.; Kamogawa, M.; Flores-Márquez, E.L.; Ramírez-Rojas, A.; Perez-Oregon, J. Improving the Estimation of the Occurrence Time of an Impending Major Earthquake Using the Entropy Change of Seismicity in Natural Time Analysis. *Geosciences* **2023**, *13*, 222. <https://doi.org/10.3390/geosciences13080222>

Academic Editors: Dimitrios Nikolopoulos and Jesus Martinez-Frias

Received: 3 July 2023

Revised: 21 July 2023

Accepted: 24 July 2023

Published: 25 July 2023



**Copyright:** © 2023 by the authors. Licensee MDPI, Basel, Switzerland. This article is an open access article distributed under the terms and conditions of the Creative Commons Attribution (CC BY) license (<https://creativecommons.org/licenses/by/4.0/>).

**Abstract:** This article is focused on a new procedure concerning a more accurate identification of the occurrence time of an impending major earthquake (EQ). Specifically, we first recapitulate that, as was recently shown [P. Varotsos et al., *Communications in Nonlinear Science and Numerical Simulation* **125** (2023) 107370], natural time analysis of seismicity supplemented with the non-additive Tsallis entropy  $S_q$  leads to a shortening of the time window of an impending major EQ. This has been shown for the Tohoku mega-EQ of magnitude  $M9$  that occurred in Japan on 11 March 2011, which is the largest event ever recorded in Japan. Here, we also show that such a shortening of the time window of an impending mainshock can be achieved for major, but smaller EQs, of the order of  $M8$  and  $M7$ . In particular, the following EQs are treated: the Chiapas  $M8.2$  EQ, which is Mexico's largest EQ for more than a century that took place on 7 September 2017 near the coast of Chiapas state in Mexico, the 19 September 2017  $M7.1$  EQ that occurred within the Mexican flat slab, and the  $M7.1$  Ridgecrest EQ on 6 July 2019 in California.

**Keywords:** natural time; earthquakes; order parameter; entropy; criticality; seismic electric signals

To the memory of the Academician Seiya Uyeda who first commented on our Chiapas earthquake results during his last visit in Athens, Greece, in November 2017.

## 1. Introduction

A new view of time, termed natural time  $\chi$  has been introduced by the first three authors in 2001, see, e.g., [1]. It has been found to be useful in various disciplines, for example it has been employed by Rundle, Turcotte, and coworkers [2–8] as a basis for a new methodology to estimate the current level of seismic risk, termed Nowcasting Earthquakes (which was recently reviewed in [9–11]). In this new view, novel dynamical features hidden behind time series in complex systems can emerge but cannot when the analysis is carried out within the frame of conventional time. Natural time analysis (NTA) enables the study of the dynamical evolution of a complex system and identifies when the system

enters a critical stage [12–14]. Earthquakes (EQs) exhibit complex correlations in time, space, and magnitude (e.g., [15–21]), and it has been widely accepted [12,22,23] that the occurrence of large earthquakes is likely associated with the proximity of crustal volumes to a critical breaking point. We clarify, however, that, as discussed by several authors, seismic activity, in general, does not require critical behavior (e.g., [24–26]) and the scaling laws of earthquakes can be derived without any reference to criticality (e.g., [27]).

The variance of natural time, i.e.,  $\kappa_1 = \langle \chi^2 \rangle - \langle \chi \rangle^2$ , is a useful quantity in identifying the approach to a critical point and in NTA of the seismicity,  $\kappa_1$  may be considered as an order parameter of seismicity [28]; see also Chapter 6 of [12,29].

NTA also revealed [30,31] that, upon studying the Olami–Feder–Christensen EQ model [32]—probably [33] the most studied non-conservative (supposedly) self-organized criticality model, see also Caruso and Kantz [34]—the entropy change of seismicity under time reversal  $\Delta S$  exhibits [12,30] an evident minimum  $\Delta S_{min}$  before large avalanches, which correspond to strong EQs. In general, it has been shown that the quantity  $\Delta S_{min}$  plays a major role upon approaching a dynamic phase transition [35] (critical point) in which the mainshock constitutes the new phase [12].

NTA revealed the identification of the epicentral area of an impending major earthquake as well as demonstrated [36,37] that the initiation of a Seismic Electric Signals (SES) activity (i.e., series of precursory variations of the electric and of the accompanying magnetic field of the Earth [38–41]) has a lead time [12] from a few weeks to  $5\frac{1}{2}$  months before a strong EQ, which almost coincides with the minimum  $\beta_{min}$  of the fluctuations  $\beta$  of the order parameter  $\kappa_1$  of seismicity.

In NTA of seismicity, the occurrence of the criticality condition  $\kappa_1 = 0.070$  [12,13,42] marks that a strong EQ is going to occur within a time window from a few hours to 1 week (up to 11 days or so, [43]). It is, of course, of major importance to shorten this time window before an impending mainshock. In particular, focusing on this period, we examine whether there exist additional variations of the entropy change  $\Delta S$  under time reversal as well as possible changes of other entropic measures. Along these lines, very recently Varotsos et al. [14] found that before the  $M9$  Tohoku EQ in Japan that occurred on 11 March 2011, which is the largest EQ ever recorded in Japan, shortly after the validity of the criticality condition  $\kappa_1 = 0.070$ , the quantity  $\Delta S$  of NTA together with the Tsallis entropy exhibited distinct simultaneous changes. Here, we extend such an investigation for three smaller EQs, i.e., the Chiapas  $M8.2$  EQ in Mexico—which is Mexico’s largest EQ for more than a century—the case of the 19 September 2017  $M7.1$  EQ that occurred within the Mexican flat slab, and the  $M7.1$  Ridgecrest EQ on 6 July 2019 in California, see Figure 1.

This work is structured as follows: In Section 2, we summarize the background of NTA and then explain in Section 3 the general procedure that we apply [12] to estimate the occurrence time of an impending mainshock. The main results of our investigation on what happens *after* the validity of the criticality condition  $\kappa_1 = 0.070$  are presented in Section 4. This section is divided into four subsections: Section 4.1 contains the results for the Chiapas  $M8.2$  EQ on 7 September 2017 and Section 4.2 the results concerning the  $M7.1$  EQ that hit central Mexico on 19 September 2017 killing more than 300 people in Morelo’s region as well as in Mexico City. In Section 4.3, the  $M7.1$  Ridgecrest EQ on 6 July 2019 in California is studied. Finally in Section 4.4 the main results for the  $M9$  Tohoku EQ in Japan on 11 March 2011 obtained in [14], as mentioned above, are recapitulated. A discussion follows in Section 5 and, finally, our main conclusions are summarized in Section 6.

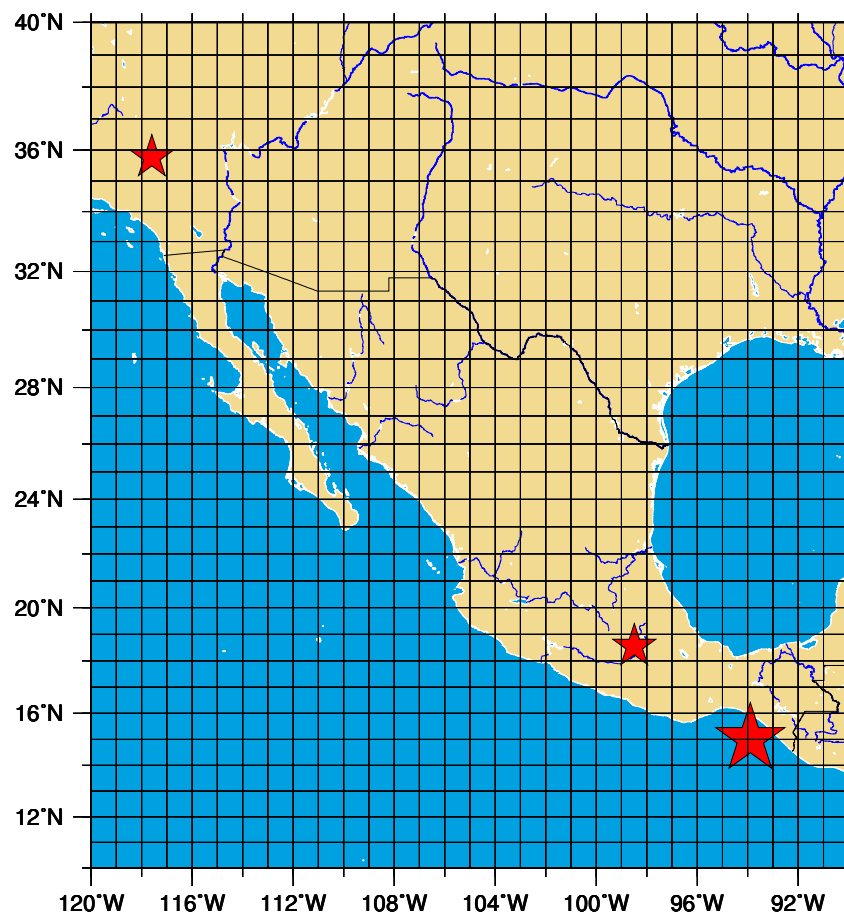


**Figure 1.** Map depicting the epicenters, from top to bottom, of the  $M7.1$  Ridgecrest EQ on 6 July 2019, the 19 September 2017  $M7.1$  EQ that occurred within the Mexican flat slab, and the Chiapas  $M8.2$  EQ in Mexico.

## 2. Natural Time Analysis: Background

Natural time analysis is based on a new concept of time that was put forward by Varotsos et al. [1], as already mentioned—see also Chapter 2 of [12] and the Appendix of [13]—and has been found useful to uncover important features hidden in complex systems time series from seismology to cardiology [44–49] and from atmospheric sciences [50,51] to complex networks [52]. Furthermore, various authors (e.g., Pasari and coworkers [53–56]) have applied the methodology of Nowcasting Earthquakes based on natural time to the contemporary earthquake hazards in several areas like West–Northwest Himalaya [53], Java Island [54], Sulawesi Island [55], and Sumatra in Indonesia [56].

For a series of  $N$  events, which actually is a temporal point pattern, see, e.g., [57], natural time serves as an index for the occurrence of the  $k$ -th event and is given by  $\chi_k = k/N$ . In NTA, the conventional interevent time is ignored, but we preserve the occurrence order and the energy  $Q_k$  of the events. For seismicity  $Q_k \propto 10^{1.5M_k}$ , where the moment magnitude  $M$  [58] is considered, see, e.g., [59]. In NTA, the evolution of the pair  $(\chi_k, p_k)$ , where  $p_k = Q_k / \sum_{k=1}^N Q_k$  is the normalized energy for the  $k$ -th event, is studied. The normalized power spectrum is defined as  $\Pi(\omega) \equiv |\Phi(\omega)|^2$  where  $\Phi(\omega) = \sum_{k=1}^N p_k \exp(i\omega\chi_k)$  and  $\omega$  denotes the angular natural frequency. Since all the moments of the distribution of the  $p_k$ , can be deduced from  $\Pi(\omega)$  in the limit  $\omega \rightarrow 0$  (see p. 130 of [12]),  $\Pi(\omega)$  is considered for  $\omega$  close to zero. The Taylor expansion of  $\Pi(\omega)$  is given by

$$\Pi(\omega) = 1 - \kappa_1\omega^2 + \kappa_2\omega^4 + \dots \quad (1)$$

where

$$\kappa_1 = \sum_{k=1}^N p_k (\chi_k)^2 - \left( \sum_{k=1}^N p_k \chi_k \right)^2 \tag{2}$$

The quantity  $\kappa_1$  corresponds to the variance  $\langle \chi^2 \rangle - \langle \chi \rangle^2$  of natural time. It is a key quantity when studying seismic catalogs [52,59–61], because Varotsos et al. [28] proved that it is the order parameter of seismicity through which one can identify when the system reaches the critical point. Note that EQs, as already mentioned in the Introduction, are widely considered [12,22,23] as critical phenomena (the mainshock being the new phase) exhibiting complex correlations in time, space and magnitude (e.g., [15,17–19,44,62,63]).

In NTA, the entropy,  $S$ , is given by:

$$S = \langle \chi \ln \chi \rangle - \langle \chi \rangle \ln \langle \chi \rangle \tag{3}$$

where  $\langle f(x) \rangle = \sum_{k=1}^N p_k f(x_k)$ . It shows [64] concavity, positivity, and Lesche stability [65,66].  $S$  is a dynamic entropy and its value  $S_u$  for a uniform ( $u$ ) distribution [12] is  $S_u = 0.096$ . The application of the time reversal operator  $\mathcal{T} p_k = p_{N-k+1}$  to  $S$ , leads to the entropy under time reversal,  $S_-$ :

$$S_- = \sum_{k=1}^N p_{N-k+1} \left( \frac{k}{N} \right) \ln \left( \frac{k}{N} \right) - \left[ \sum_{k=1}^N p_{N-k+1} \left( \frac{k}{N} \right) \right] \ln \left[ \sum_{k=1}^N p_{N-k+1} \left( \frac{k}{N} \right) \right] \tag{4}$$

The difference,  $\Delta S = S - S_-$ , represents an important quantity with a physical meaning studied in detail in [12,30,35,67]. As already mentioned,  $\Delta S$  is a key parameter, which may determine the approach to a dynamic phase transition [12,35,68].

The fluctuations of  $\Delta S$  are studied as follows: Using a moving window of length  $i$  (number of successive events) sliding through the EQ catalog, the time series of  $S_i$  and  $(S_-)_i$  are obtained. By means of the standard deviation  $\sigma(\Delta S_i)$  of the time series of  $\Delta S_i \equiv S_i - (S_-)_i$ , the complexity measure  $\Lambda_i$  [12,45,69] is defined

$$\Lambda_i = \frac{\sigma(\Delta S_i)}{\sigma(\Delta S_{100})}, \tag{5}$$

where the denominator corresponds [69] to the standard deviation  $\sigma(\Delta S_{100})$  of the time series of  $\Delta S_i$  with  $i = 100$  events. The quantity  $\Lambda_i$  quantifies how the statistics of  $\Delta S_i$  time series is changed upon increasing the scale from 100 EQs to a longer scale, e.g.,  $i = 500$  EQs.

### 3. Identification of the Occurrence Time of the Impending Mainshock

The relevant procedure has been reviewed by Varotsos et al. [70]. For SES activities has been shown [1,12] that:

$$\Pi(\omega) = \frac{18}{5\omega^2} - \frac{6\cos\omega}{5\omega^2} - \frac{12\sin\omega}{5\omega^3}, \tag{6}$$

which simplifies to:

$$\Pi(\omega) \approx 1 - 0.07\omega^2 \tag{7}$$

when  $\omega \rightarrow 0$ . Equation (7), when considering Equation (1), results in

$$\kappa_1 = 0.070. \tag{8}$$

The above critical condition has been proven for several EQ models (see, e.g., [12,42]), as well as it has been found of usefulness in a variety of other EQ precursory phenomena [71–79].

The NTA of seismicity in the future epicentral area begins upon the starting of SES activity [28,43,80] because the latter is emitted when the focal area enters the critical stage [12,13,81]. Hence, we form EQ time series in natural time for the future epicentral

area, each time when a small EQ of magnitude  $M$  exceeds a certain threshold  $M_{\text{thres}}$ . The value of  $\Pi(\omega)$  for  $\omega \rightarrow 0$  and the one of  $\kappa_1$  for each of the EQ time series is estimated and compared to that of Equation (6) for  $\omega \in [0, \pi]$ . Furthermore, the two entropies  $S$  and  $S_-$  are also calculated. The established criteria to assure a true coincidence of the EQ time series with that of critical state are the following [12,28,82,83]: (i) The “average” distance  $\langle D \rangle$  between the curves of  $\Pi(\omega)$  of the evolving seismicity and Equation (6) should be  $\langle D \rangle < 10^{-2}$ . (ii) The final approach of the evolving  $\Pi(\omega)$  to that of Equation (6) must be from below as depicted by the arrow in Figure 7.1 of [12] (as well as in Figure 5 of [84]). This means that, before strong EQs,  $\kappa_1$  finally approaches from above that of the critical state, i.e.,  $\kappa_1 = 0.070$ . (iii) The entropies  $S$  and  $S_-$  should be less than  $S_u$  at the coincidence. (iv) The time of the true coincidence should not change significantly upon varying  $M_{\text{thres}}$ , since the process (critical dynamics) has to be self-similar.

#### 4. Results

In Section 4.1, we mainly focus on the improvement of the identification of the occurrence time of the  $M8.2$  Chiapas EQ on 7 September 2017 in Mexico, which has been first attempted by Sarlis et al. [60], and in Section 4.2, we present the results for the  $M7.1$  EQ on 19 September 2017 in the Mexican flat slab. In Section 4.3, we treat the case of the  $M7.1$  Ridgecrest EQ on 6 July 2019 in California and finally, in Section 4.4 we summarize the results for the  $M9$  Tohoku EQ on 11 March 2011 that, as mentioned, have been published by Varotsos et al. [14].

##### 4.1. Results on the $M8.2$ Chiapas EQ

The following result was deduced by the NTA of the Mexican seismicity from 1 January 1988 until the  $M8.2$  Chiapas EQ on 7 September 2017 by using sliding natural time window lengths consisting of a number of events that would occur in a few months, which is approximately equal with the average value of the lead time of SES activities. Almost 1.5 months before the  $M8.2$  Chiapas EQ the minimum  $\beta_{\text{min}}$  was found approximately on 27 July 2017 as the deepest minimum during the almost thirty year period investigated [60] (cf. while  $\Delta S_{\text{min}}$  has been earlier observed, i.e., on 14 June 2017, as previously mentioned).

Second, we make use of the experimental fact [37] that an SES activity initiates almost simultaneously with  $\beta_{\text{min}}$ . Hence, an SES activity should have started approximately around 27 July 2017.

Third, we now plot in Figure 2 the quantity  $\Delta S$  (a) and the Tsallis non-additive entropy  $S_q$  [85–91] (b) versus the conventional time in the Chiapas region (see Figure 2 of [31]) during the period almost one week before the  $M8.2$  EQ. The seismic data analyzed come from the seismic catalog of the National Seismic Service (SSN) of the Universidad Nacional Autónoma de México ([www.ssn.unam.mx](http://www.ssn.unam.mx), accessed on 23 November 2017) and to assure catalog completeness a magnitude threshold  $M_{\text{thres}} = 3.5$  has been imposed as in [31]. Starting from the above date of  $\beta_{\text{min}}$  on 27 July 2017, and considering the seismicity in Chiapas area (which is the candidate area), we find that the criticality condition  $\kappa_1 = 0.070$  had been fulfilled (together with the fact that the aforementioned criteria for recognizing a true coincidence were satisfied) from 21:08 CDT (=UTC-5) on 5 September 2017 until 16:06 CDT on 6 September 2017. This latter period is shaded in Figure 2. An additional inspection of this figure reveals the following: Approximately on 02:05 CDT on 7 September 2017 a simultaneous change appears both on  $\Delta S$  of NTA, see Figure 2a, and on  $S_q$ , see Figure 2b, i.e., almost 10 h after the aforementioned validity of the criticality condition  $\kappa_1 = 0.070$ . It is challenging that, after the system entered the critical stage, both these quantities, i.e.,  $\Delta S$  and  $S_q$ , exhibit an almost transient change of similar shape upon the occurrence of a  $M4.8$  EQ on 7 September 2017. The  $M8.2$  Chiapas EQ occurred at 23:49 CDT on 7 September 2017, i.e., several hours later.

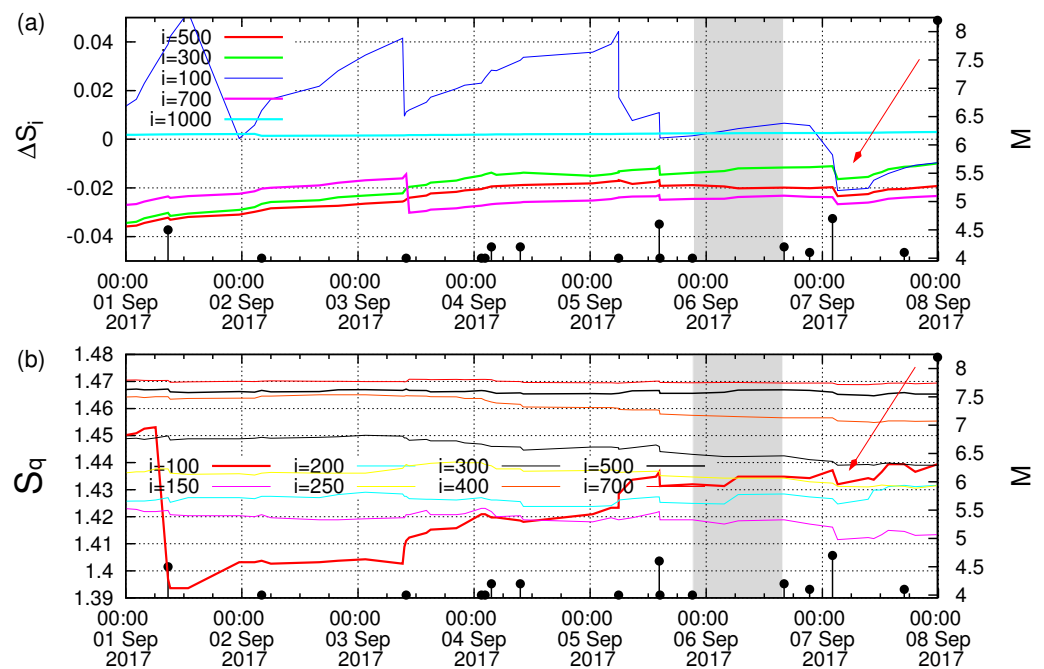


**Figure 2.** Plot of  $\Delta S$  in NTA (a) and the Tsallis entropy  $S_q$  (b) versus the conventional time in the Chiapas region in Mexico before the occurrence of the M8.2 EQ on 7 September 2017. The red arrows indicate the simultaneous change of  $\Delta S_i$  and  $S_q$  after the validity of the criticality condition  $\kappa_1 = 0.070$ . The shaded region corresponds to the period during which this criticality condition is obeyed [60].

Fourth, in view of the above observation (i.e., that after the system entered the critical stage, there exists the aforementioned similarity between the changes of the quantities  $\Delta S$  and  $S_q$ ), we are inspired to examine whether the precursory minimum  $\Delta S_{min}$  on 14 June 2017 also exists in  $S_q$ . Hence, we plot in Figure 3b the  $S_q$  versus the conventional time for various scales from  $i = 100$  to 700 events in the Chiapas region from 10 June 2017 until the M8.2 EQ on 7 September 2017. We find that there exists a minimum for the shorter scales which can be better seen in Figure 3c when we plot  $S_q$  versus the conventional time, but in an expanded scale. An inspection of the latter figure shows that the precursory minimum on 14 June 2017 we reported long ago in [31] on the basis of  $\Delta S$  (see also Figures 4 and 5) also appears in  $S_q$ . We emphasize, however, that  $\Delta S$  and  $S_q$  are *not* equivalent. In particular, the minimum observed when  $\Delta S$  is used is *unique* during the whole period studied (see [31]), which is *not* the case of  $S_q$ , see Figure 3a where upon using  $S_q$  several minima appear. In other words, only when employing  $\Delta S$  a unique minimum  $\Delta S_{min}$  can be distinguished on 14 June 2017, while upon using  $S_q$  alone we cannot isolate—among several minima in Figure 3a—which is of truly precursory nature.

Fifth, in [69] we found that the change of the complexity measure  $\Lambda_i$ , i.e.,  $\Delta\Lambda_i(\equiv \Lambda_i(t) - \Lambda_i(t_{EQ}))$ , upon the occurrence of the minimum  $\Delta S_{min}$ , showed increased fluctuations of the entropy change under time reversal that obeyed the seminal work on phase transitions by Lifshitz and Slyozov [92] and independently by Wagner [93] (LSW). These works showed that the characteristic size of the minority phase droplets grows with conventional time  $t$  as  $t^{1/3}$ . Hence, we now turn to investigate whether it also holds for the Tsallis entropy  $S_q$ . In Figure 6, we plot the quantity  $\Delta S_q = (S_q)_0 - S_q$  of the Tsallis non-additive entropy versus  $t - t_0$  in the Chiapas region in Mexico before the occurrence of the M8.2 EQ on 7 September 2017 and  $t_0 = 0.011$  days just after the M7.0 Guatemala EQ on 14 June 2017.  $(S_q)_0$  corresponds to the value of  $S_q$  just before the latter EQ. Figure 6 reveals that  $\Delta S_q$  obeys the  $t^{1/3}$  time growth of the characteristic size of the minority phase droplets of the seminal LSW phase transition theory since the slope of the three straight lines drawn in this log-log plot is 1/3.

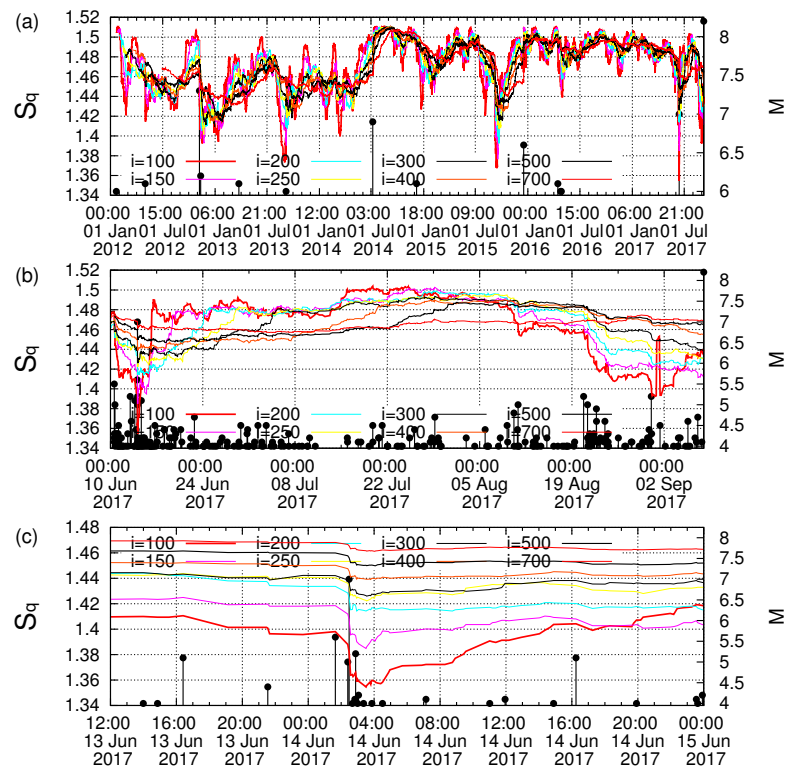


**Figure 3.** Plot of  $S_q$  versus the conventional time for various scales, i.e.,  $i = 100$  to 700 events, in Chiapas region from 1 January 2012 (a) or from 10 June 2017 (b) until the M8.2 Chiapas EQ. In (c), we plot an excerpt of (b), but in an expanded time scale during only the period in which  $\Delta S$  in NTA showed a minimum on 14 June 2017 as described in [31]. See also Figures 4 and 5.

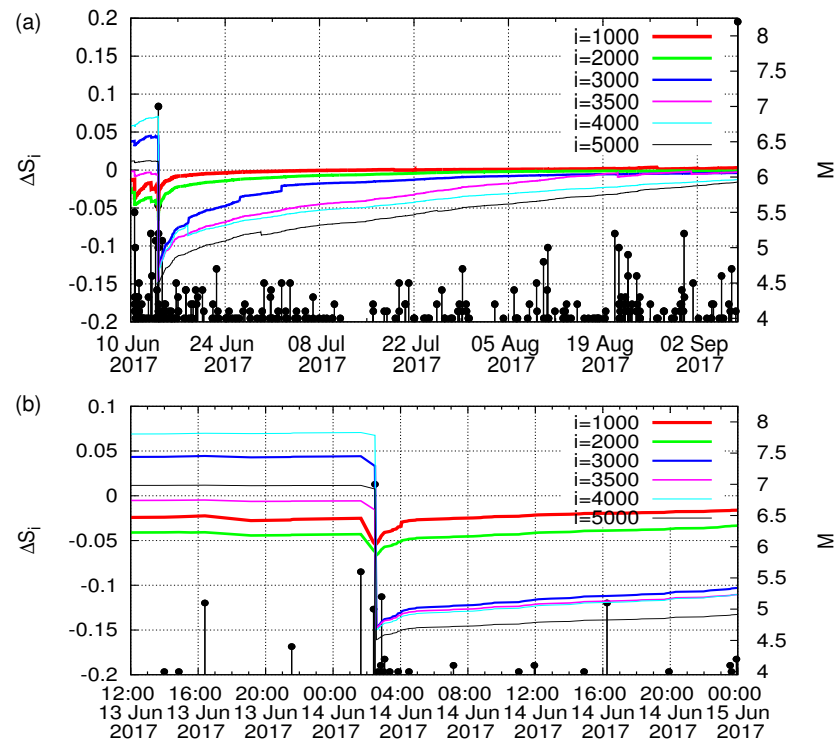


**Figure 4.** The same as Figure 2a, i.e., plot of  $\Delta S_i$  versus the conventional time, but for the following periods: from 10 June 2017 until the M8.2 Chiapas EQ (a,b) in the expanded time scale from 12:00 CDT on 13 June until 00:00 CDT on 15 June 2017.

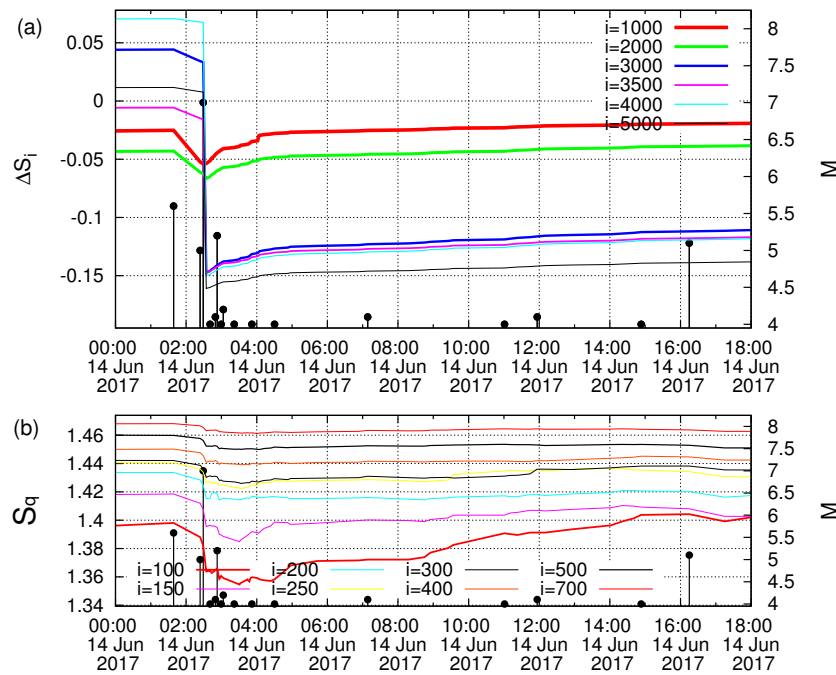


**Figure 5.** The same as Figure 2, but in expanded scale for the following periods: (a)  $\Delta S_i$  from 00:00 CDT on 14 June 2017 until 18:00 CDT on 14 June 2017; (b)  $S_q$  from 00:00 CDT on 14 June 2017 until 18:00 CDT on 14 June 2017.

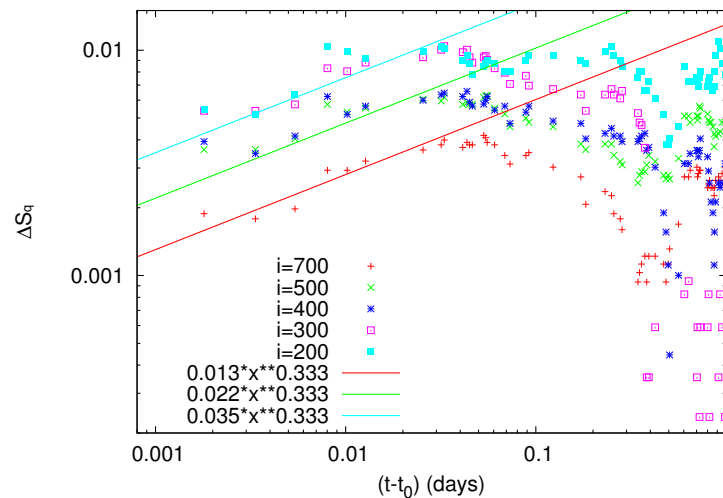


**Figure 6.** Plot of  $\Delta S_q = (S_q)_0 - S_q$  of the Tsallis non-additive entropy versus  $t - t_0$ , where  $t_0 = 0.011$  days, in Chiapas region in Mexico before the  $M8.2$  EQ occurrence on 7 September 2017 and just after the  $M7.0$  Guatemala EQ on 14 June 2017.  $S_0(q)$  corresponds to the value of  $S_q$  just before the latter EQ. The slope of the straight lines of this log-log plot is  $1/3$  which reveals the  $t^{1/3}$  behavior of the LSW theory (see the text).

**4.2. Results on the  $M7.1$  EQ on 19 September 2017 within the Mexican Flat Slab**

The first results on the NTA on this EQ have been published by Flores-Márquez et al. [84]. In short, the seismicity in the flat slab region has been analyzed in natural time from 1995 until the  $M7.1$  EQ occurrence in 2017 by investigating the entropy change  $\Delta S$  under time reversal together with the variability  $\beta$  of the order parameter of seismicity. The EQ catalog of SSN from 1 September 1995 until 24 September 2017, was used [84]. Considering the area of the flat slab and taking just the EQs with epicenters situated between 40 and 60 km of Moho depths, Flores-Márquez et al. [84] plot their spatial distribution in the upper panel of their Figure 2. To assure catalog completeness, a magnitude threshold

$M_{\text{thres}} = 3.5$  was imposed after studying the cumulative frequency magnitude distribution as in [84]. The quantity  $\Delta S$  was minimized on 21 June 2017 which is approximately one week after the minimum  $\Delta S_{\text{min}}$  that preceded the  $M8.2$  Chiapas EQ on 7 September 2017. In particular, a clear minimum  $\Delta S_{\text{min}}$  appeared on 21 June 2017 upon a  $M4.8$  EQ occurrence, approximately 3 months before the  $M7.1$  EQ occurrence on 19 September 2017. A  $\beta$  minimum was also observed during the period February–March 2017. In addition, it was shown that, after  $\Delta S_{\text{min}}$ , the seismicity order parameter  $\kappa_1$  starts diminishing by gradually approaching the critical value 0.070 around the end of August and the beginning of September 2017.

The criteria that assured the true coincidence of the EQ time series with that of critical state [12,82] have been checked during the period after 21 February 2017. This was obtained on the basis of the variability minimum which was unique during the whole period studied. A more detailed inspection uncovers that the second criterion for the true coincidence starts to be obeyed on 21 June 2017: The order parameter  $\kappa_1$  after 21 June 2017 starts diminishing from values  $\kappa_1 > 0.070$  and finally approaching from above the value  $\kappa_1 = 0.070$  around the end of August and the beginning of September (this period is shaded in Figure 7). In other words,  $\Pi(\omega)$  starts to follow the behavior indicated by the red arrow observed in Figure 5 of [84] on the date that  $\Delta S_i$  showed the minimum, i.e., just after 21 June 2017.

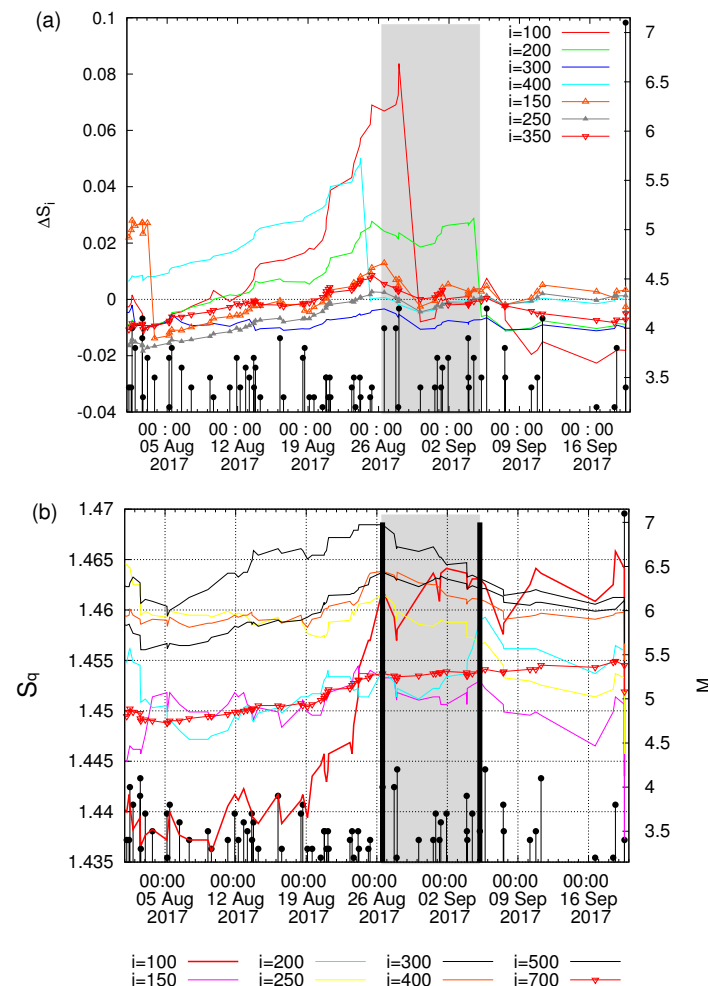


**Figure 7.** Plot of  $\Delta S$  in NTA (a) and the Tsallis entropy  $S_q$  (b) versus the conventional time (CDT) before the occurrence of the  $M7.1$  EQ on 19 September 2017 within the Mexican flat slab. The shaded region corresponds to the period during which the criticality condition  $\kappa_1 = 0.070$  is obeyed [84].

The shaded area in Figure 7 indicates the period during which the condition  $\kappa_1 = 0.070$  holds. After this period and in particular during the last few days before the  $M7.1$  EQ occurrence,

a similarity of  $\Delta S_i$  and  $S_q$  emerges in Figure 7. In this Figure, for better visualization of their changes the threshold  $M_{\text{thres}} = 3.2$  has been adopted. Specifically, a number of transient changes of similar shape on both quantities appear, see for example the local minima of both  $\Delta S_i$  and  $S_q$  in Figure 7a,b upon the occurrence of an event on 16 September 2017, as well as the local maxima upon the occurrence of a  $M3.8$  EQ on 18 September 2017.

#### 4.3. Results on the $M7.1$ Ridgecrest EQ on 6 July 2019 in California

Three EQs of moment magnitudes  $M = 6.4, 5.4,$  and  $7.1$ , north and northeast of the town of Ridgecrest, California, occurred in 2019. The latter, being the mainshock, was the most powerful EQ in the California state in 20 years, i.e., after the Hector Mine EQ in 1999. Specifically, at 17:33 UTC on 4 July 2019, a  $M6.4$  foreshock occurred followed by a series of additional EQs, the strongest of which was a  $M5.4$  at 11:07 UTC on 5 July. Finally, at 03:20 UTC on 6 July, a larger  $M7.1$  EQ occurred in the Ridgecrest area followed by thousands of aftershocks. A map depicting all the  $M \geq 2.0$  EQs reported by the Southern California Earthquake Center (SCEC) since 1 January 2004 is shown in Figure 9.7 of [13]. The EQ catalog of SCEC, available at [http://service.scedc.caltech.edu/ftp/catalogs/SCEC\\_DC/](http://service.scedc.caltech.edu/ftp/catalogs/SCEC_DC/), was used (accessed on 1 August 2019). Following previous work [94], we considered a magnitude threshold  $M_{\text{thres}} = 2.0$  and focused in the analysis of seismicity within the geographic polygon shown in Figure 1 of [95] that covers the Southern California Seismic Network reporting area for local events. The  $\beta_W$  values have been computed for sliding natural time window lengths  $W = 200, 250, 300, 350, 400, 450,$  and  $500$  events and plotted in Figure 9.8 of [13] along with the Detrended Fluctuation Analysis [96] (DFA) exponent  $\alpha_{300}$ —deduced from the EQ magnitude time series consisting of 300 events—versus the conventional time since 1 January 2004 until the  $M7.1$  Ridgecrest EQ occurrence on 6 July 2019.

As can be seen in Figure 9.9a of [13], a few months before the 2019  $M7.1$  Ridgecrest EQ all  $\beta_W$  values exhibited an initial decrease after approximately 10 February 2019 and gradually approached their minimum values from 29 May to 5 June 2019. When these minima are reached, the corresponding DFA exponent  $\alpha_{300}$  values were above  $\alpha = 0.5$  (pointing to the presence of long-range correlations), as can be visualized in Figure 9.9b of [13]. In other words, the temporal correlations between EQ magnitudes deduced by means of DFA revealed that, while on 5 June 2019 the fluctuations of the order parameter of seismicity exhibited a minimum  $\beta_{\text{min}}$  showing long-range correlations ( $\alpha_{300} \approx 0.6$ ), they have been destroyed before the  $M7.1$  EQ since a behavior close to random ( $\alpha = 0.5$ ) and subsequently anticorrelated ( $\alpha < 0.5$ ) was observed almost upon of the  $M6.4$  EQ occurrence on 4 July 2019.

Studying natural time analysis of seismicity from the minimum  $\beta_{\text{min}}$  of the variability on 5 June 2019, we find [59] that the criticality condition  $\kappa_1 = 0.070$  is obeyed at 22:41 UTC on 2 July 2019 almost 3 days before the  $M6.4$  EQ occurrence. By the same token as in Sections 4.1 and 4.2, we now depict in Figure 8 the quantities  $\Delta S_i$  and  $S_q$  versus the conventional time. This figure shows that transient changes of these quantities start upon the  $M5.4$  EQ occurrence on 5 July 2019 (marked by the red arrows “start”) and end in the beginning of 6 July 2019 (marked also with the red arrows “end”) upon a  $M3.46$  EQ occurrence at 00:13 UTC (see Figure 3 of [59]), almost 3 h before the  $M7.1$  Ridgecrest EQ. In other words, there exist transient changes on both quantities  $\Delta S_i$  and  $S_q$ , which start as well end upon the occurrence of the events  $M5.4$  EQ on 5 July and the  $M3.46$  EQ on 6 July, respectively.

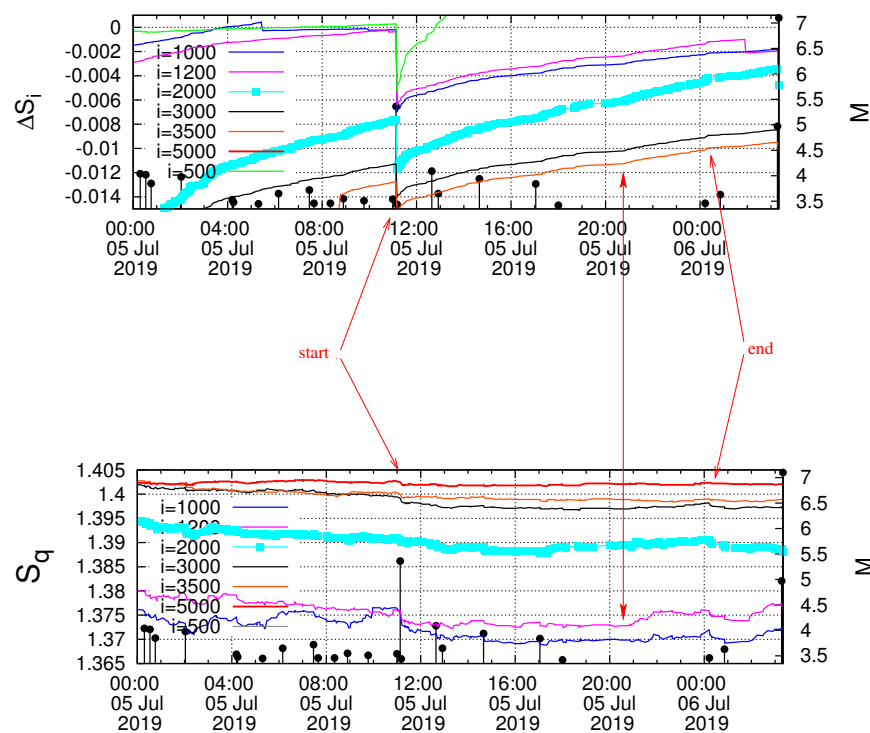


**Figure 8.** The quantities  $\Delta S_i$  and  $S_q$  versus the conventional time before the  $M7.1$  Ridgecrest EQ. Transient changes of these quantities *start* upon the  $M5.4$  EQ occurrence on 5 July 2019 (marked by the red arrows “start”) and *end* in the beginning of 6 July 2019 (they are also marked with the red arrows “end”) upon a  $M3.46$  EQ occurrence at 00:13 UTC, almost 3 h before the  $M7.1$  Ridgecrest EQ occurrence. The criticality condition  $\kappa_1 = 0.070$  was obeyed [59] at 22:41UTC on 2 July 2019 that precedes the period depicted in Figure.

**4.4. Results on the  $M9$  Tohoku EQ Occurrence on 11 March 2011**

Approximately a day before the  $M9$  Tohoku EQ occurrence on 11 March 2011 the following results have been obtained [97]: NTA revealed that the order parameter  $\kappa_1$  of seismicity, and in particular from 08:36 to 13:14 LT on 10 March 2011, obeyed the critical condition  $\kappa_1 = 0.070$  which signals that the main shock is going to occur within the next few days (up to around 11 days or so [43]). The data come from the Japan Meteorological Agency (JMA) seismic catalog upon setting a magnitude threshold  $M_{\text{thres}} = 3.5$  to assure data completeness as in [80]. The following two important findings have been observed [97] just before this period: First, the Tsallis entropic index  $q$  exhibited distinct changes at 03:16 LT and 06:24 LT on 10 March 2011. Second, upon the  $M7.3$  foreshock occurrence on 9 March 2011, a prominent increase  $\Delta q$  of the Tsallis entropic index  $q$  was observed that showed a scaling behavior with a characteristic exponent  $1/3$  which conforms to the seminal work by LSW on phase transitions predicting that the time growth of minority phase droplets grows with time  $t$  as  $t^{1/3}$ . As for the prefactor  $A$  in the relation  $\Delta q = A(t - t_0)^c$  of [97] of LSW theory, it increases when the scale  $i$  decreases, see Figure 3 of [97], in contrast to the complexity measure  $\Delta_i$  quantifying the  $\Delta S$  fluctuations for which the LSW prefactor  $A$  increases upon increasing the scale  $i$  [98].

The following additional results have just been deduced by Varotsos et al. [14]: After the above mentioned period from 08:36 at 13:14 LT on 10 March 2011 in which the system entered the critical stage, simultaneous changes appear at 18:00 and 20:00 LT on 10 March 2011 on both the quantity  $\Delta S$  (see Figure 3a,b of Ref. [14]) and the Tsallis entropy  $S_q$  (see Figure 3c,d of Ref. [14]). These simultaneous changes can be seen with much difficulty when the computation is made in the entire Japanese region, but are evident when computed in the future epicentral region. A few hours later, the changes  $\Delta \Delta_i$  of all the complexity measures  $\Delta \Delta_{2000}$ ,  $\Delta \Delta_{3000}$  and  $\Delta \Delta_{4000}$  show a simultaneous variation almost

around 00:00 LT on 11 March 2011, i.e., almost several hours before the *M9* EQ occurrence (see Figure 9 of Ref. [98]).

## 5. Discussion

Following [99], fluctuations are the dominant feature of criticality and their presence is spatially boundless while their duration is finite as they offer an ever-changing landscape. Their appearance is such that the critical state looks the same on any length scale, i.e., it is statistically scale invariant.

The fluctuations of a second order phase transition are usually studied by means of the Landau free energy in order to investigate the order parameter fluctuations and the validity of mean field theory. Close enough to the critical point, the fluctuations will become as important as the mean. The region near the critical point where fluctuations are important is known as the critical region. Close enough to the critical point, mean field theory breaks down and fluctuations are always important. The benchmark of the critical state is, as mentioned, its self similarity expressed by spatial and temporal scale invariance of correlations.

Concerning the interrelation between the order parameter fluctuations and non-extensivity, Tsallis et al. [100] showed that for asymptotically scale-invariant systems, it is  $S_q$  with  $q \neq 1$ , and not  $S_{BG}$  (cf. the subscript *BG* stands for Boltzmann–Gibbs entropy in which  $q = 1$ ), the entropy which matches standard Clausius-like, prescriptions of classical thermodynamics. They also noted that the subtle case of thermodynamic critical points, where correlations at all scales exist. There, we can still refer to  $S_{BG}$ , but it exhibits singular behavior which is due to the fractal structure of the correlation clusters existing at critical points; an instructive description in non-extensive terms of such situations has been advanced in [101,102] the results of which show [102] that the departure from *BG* statistics and the applicability of  $q$ -statistics is due in part to the presence of the long range correlations in space and in time taking place at criticality. This sheds light on the point why we investigate here whether a simultaneous appearance in the changes of  $\Delta S$  with those in  $S_q$  is observed after the system enters the critical stage. We recall, as mentioned in the Introduction, that  $\Delta S$  plays a major role upon approaching a dynamic phase transition (critical point) in which the mainshock constitutes the new phase.

Finally, we note that since both  $\Delta S$  and  $S_q$  are experimentally stable [65,66], as shown in [64,103], respectively, we do not expect the above findings to change within a plausible experimental error in the determination of the EQ magnitudes.

## 6. Summary and Main Conclusions

For the case of the *M8.2* Chiapas EQ on 7 September 2017:

(a) The  $\Delta S_{min}$  appears on 14 June 2017 almost three months in advance. As for the validity of the criticality condition  $\kappa_1 = 0.070$ , the corresponding criteria for the true coincidence hold from 21:08 CDT on 5 September 2017 until 16:06 CDT on 6 September 2017.

(b) After the latter period,  $\Delta S$  exhibits a transient change several hours before the mainshock occurrence being strikingly similar in shape to an  $S_q$  change, see Figure 2.

(c) Both measures  $\Delta \Lambda_i$  and  $\Delta S_q$  obey the seminal LSW theory of phase transitions according to which the characteristic size of the minority phase droplets grows with the time as  $t^{1/3}$ . This, however, should not be misinterpreted that these measures are equivalent for the reason that will be explained at the end of this Section.

We now proceed to the results obtained here for the *M7.1* EQ within the Mexican flat slab on 19 September 2017: After the validity of the criticality condition  $\kappa_1 = 0.070$  lasting around from the end of August 2017 until the beginning of September 2017, we found transient changes of  $\Delta S$ , accompanied by simultaneous changes of  $S_q$  from 11 September 2017 until 18 September 2017, i.e., almost one day before the *M7.1* EQ occurrence within the Mexican flat slab, see Figure 7.

More or less similar phenomena appear before the *M7.1* Ridgecrest EQ. In particular, transient changes  $\Delta S_i$  accompanied by simultaneous changes of  $S_q$  start upon the *M5.4* EQ

on 5 July 2019, i.e., several hours before the mainshock, until just a few hours before the M7.1 Ridgecrest EQ.

Finally, we recall that in [14] we have shown that shortening of the time window of the impending 2011 Tohoku M9 EQ has been achieved to several hours by combining NTA of seismicity,  $\Delta S$ , and the Tsallis entropy.

After recapitulating the aforementioned results, we emphasize the following:

There exists a superiority of NTA compared to  $S_q$  as it emerges from the following facts: The  $\Delta S$  minimum observed before the M8.2 Chiapas EQ on 14 June 2017, see Figure 7 of [31], is *unique* during the whole period studied. This is *not*, however, the case for the  $S_q$ , for example, see Figure 3c,d of [14] and Figure 3a where upon using  $S_q$  several minima appear, none of which can be distinguished as precursory minimum when using  $S_q$  alone. On the other hand, the minimum  $\Delta S_{min}$  (see also Figure 8 of [31]) being accompanied by an evident increase in the complexity measure  $\Lambda_i$  can be uniquely distinguished as precursor.

**Author Contributions:** Conceptualization, P.A.V., N.V.S., E.S.S., T.N., and M.K.; methodology, P.A.V., N.V.S., E.S.S., T.N., M.K., E.L.F.-M., and A.R.-R.; software, N.V.S., E.S.S., and J.P.-O.; validation, T.N., M.K., E.L.F.-M., A.R.-R., and J.P.-O.; formal analysis, P.A.V., N.V.S., and E.S.S.; investigation, P.A.V., N.V.S., E.S.S., T.N., M.K., E.L.F.-M., A.R.-R., and J.P.-O.; resources, N.V.S., E.S.S., E.L.F.-M., A.R.-R., and J.P.-O.; data curation, E.S.S., E.L.F.-M., A.R.-R., and J.P.-O.; writing—original draft preparation, P.A.V., N.V.S., and E.S.S.; writing—review and editing, P.A.V., N.V.S., E.S.S., T.N., M.K., E.L.F.-M., A.R.-R., and J.P.-O.; visualization, E.S.S. and N.V.S.; supervision, P.A.V.; project administration, P.A.V. All authors have read and agreed to the published version of the manuscript.

**Funding:** This research received no external funding.

**Institutional Review Board Statement:** Not applicable.

**Informed Consent Statement:** Not applicable.

**Data Availability Statement:** All seismological data used are publicly available as described in [59,60,80,84].

**Conflicts of Interest:** The authors declare no conflict of interest.

## References

1. Varotsos, P.A.; Sarlis, N.V.; Skordas, E.S. Long-range correlations in the electric signals that precede rupture. *Phys. Rev. E* **2002**, *66*, 011902. [[CrossRef](#)] [[PubMed](#)]
2. Rundle, J.B.; Turcotte, D.L.; Donnellan, A.; Grant Ludwig, L.; Luginbuhl, M.; Gong, G. Nowcasting earthquakes. *Earth Space Sci.* **2016**, *3*, 480–486. [[CrossRef](#)]
3. Rundle, J.B.; Luginbuhl, M.; Giguere, A.; Turcotte, D.L. Natural Time, Nowcasting and the Physics of Earthquakes: Estimation of Seismic Risk to Global Megacities. *Pure Appl. Geophys.* **2018**, *175*, 647–660. [[CrossRef](#)]
4. Luginbuhl, M.; Rundle, J.B.; Hawkins, A.; Turcotte, D.L. Nowcasting Earthquakes: A Comparison of Induced Earthquakes in Oklahoma and at the Geysers, California. *Pure Appl. Geophys.* **2018**, *175*, 49–65. [[CrossRef](#)]
5. Luginbuhl, M.; Rundle, J.B.; Turcotte, D.L. Natural Time and Nowcasting Earthquakes: Are Large Global Earthquakes Temporally Clustered? *Pure Appl. Geophys.* **2018**, *175*, 661–670. [[CrossRef](#)]
6. Rundle, J.B.; Giguere, A.; Turcotte, D.L.; Crutchfield, J.P.; Donnellan, A. Global Seismic Nowcasting with Shannon Information Entropy. *Earth Space Sci.* **2019**, *6*, 191–197. [[CrossRef](#)]
7. Rundle, J.B.; Luginbuhl, M.; Khapikova, P.; Turcotte, D.L.; Donnellan, A.; McKim, G. Nowcasting Great Global Earthquake and Tsunami Sources. *Pure Appl. Geophys.* **2019**, *177*, 359–368. [[CrossRef](#)]
8. Fildes, R.A.; Turcotte, D.L.; Rundle, J.B. Natural time analysis and nowcasting of quasi-periodic collapse events during the 2018 Kilauea volcano eruptive sequence. *Earth Space Sci.* **2022**, *9*, e2022EA002266. [[CrossRef](#)]
9. Rundle, J.B.; Donnellan, A.; Fox, G.; Crutchfield, J.P.; Granat, R. Nowcasting Earthquakes: Imaging the Earthquake Cycle in California with Machine Learning. *Earth Space Sci.* **2021**, *8*, e2021EA001757. [[CrossRef](#)]
10. Rundle, J.B.; Donnellan, A.; Fox, G.; Crutchfield, J.P. Nowcasting Earthquakes by Visualizing the Earthquake Cycle with Machine Learning: A Comparison of Two Methods. *Surv. Geophys.* **2022**, *43*, 483–501. [[CrossRef](#)]
11. Rundle, J.; Stein, S.; Donnellan, A.; Turcotte, D.L.; Klein, W.; Saylor, C. The Complex Dynamics of Earthquake Fault Systems: New Approaches to Forecasting and Nowcasting of Earthquakes. *Rep. Prog. Phys.* **2021**, *84*, 076801. [[CrossRef](#)]

12. Varotsos, P.A.; Sarlis, N.V.; Skordas, E.S. *Natural Time Analysis: The New View of Time. Precursory Seismic Electric Signals, Earthquakes and Other Complex Time-Series*; Springer: Berlin/Heidelberg, Germany, 2011. [[CrossRef](#)]
13. Varotsos, P.A.; Sarlis, N.V.; Skordas, E.S. *Natural Time Analysis: The New View of Time, Part II. Advances in Disaster Prediction Using Complex Systems*; Springer Nature: Cham, Switzerland, 2023. [[CrossRef](#)]
14. Varotsos, P.; Sarlis, N.; Skordas, E.; Nagao, T.; Kamogawa, M. Natural time analysis together with non-extensive statistical mechanics shorten the time window of the impending 2011 Tohoku M9 earthquake in Japan. *Commun. Nonlinear Sci. Numer. Simul.* **2023**, *125*, 107370. [[CrossRef](#)]
15. Huang, Q. Seismicity changes prior to the Ms8.0 Wenchuan earthquake in Sichuan, China. *Geophys. Res. Lett.* **2008**, *35*, L23308. [[CrossRef](#)]
16. Huang, Q. Retrospective investigation of geophysical data possibly associated with the Ms8.0 Wenchuan earthquake in Sichuan, China. *J. Asian Earth Sci.* **2011**, *41*, 421–427. [[CrossRef](#)]
17. Telesca, L.; Lovallo, M. Non-uniform scaling features in central Italy seismicity: A non-linear approach in investigating seismic patterns and detection of possible earthquake precursors. *Geophys. Res. Lett.* **2009**, *36*, L01308. [[CrossRef](#)]
18. Lennartz, S.; Livina, V.N.; Bunde, A.; Havlin, S. Long-term memory in earthquakes and the distribution of interoccurrence times. *EPL (Europhys. Lett.)* **2008**, *81*, 69001. [[CrossRef](#)]
19. Lennartz, S.; Bunde, A.; Turcotte, D.L. Modelling seismic catalogues by cascade models: Do we need long-term magnitude correlations? *Geophys. J. Int.* **2011**, *184*, 1214–1222. [[CrossRef](#)]
20. Rundle, J.B.; Holliday, J.R.; Graves, W.R.; Turcotte, D.L.; Tiampo, K.F.; Klein, W. Probabilities for large events in driven threshold systems. *Phys. Rev. E* **2012**, *86*, 021106. [[CrossRef](#)]
21. Xiong, Q.; Brudzinski, M.R.; Gossett, D.; Lin, Q.; Hampton, J.C. Seismic magnitude clustering is prevalent in field and laboratory catalogs. *Nat. Commun.* **2023**, *14*, 2056. [[CrossRef](#)]
22. Carlson, J.M.; Langer, J.S.; Shaw, B.E. Dynamics of earthquake faults. *Rev. Mod. Phys.* **1994**, *66*, 657–670. [[CrossRef](#)]
23. Holliday, J.R.; Rundle, J.B.; Turcotte, D.L.; Klein, W.; Tiampo, K.F.; Donnellan, A. Space-Time Clustering and Correlations of Major Earthquakes. *Phys. Rev. Lett.* **2006**, *97*, 238501. [[CrossRef](#)] [[PubMed](#)]
24. Bowman, D.D.; Ouillon, G.; Sammis, C.G.; Sornette, A.; Sornette, D. An observational test of the critical earthquake concept. *J. Geophys. Res. Solid Earth* **1998**, *103*, 24359–24372. [[CrossRef](#)]
25. Sornette, D.; Ouillon, G. Dragon-kings: Mechanisms, statistical methods and empirical evidence. *Eur. Phys. J. Spec. Top.* **2012**, *205*, 1–26. [[CrossRef](#)]
26. Nandan, S.; Ram, S.K.; Ouillon, G.; Sornette, D. Is Seismicity Operating at a Critical Point? *Phys. Rev. Lett.* **2021**, *126*, 128501. [[CrossRef](#)] [[PubMed](#)]
27. Zaccagnino, D.; Telesca, L.; Doglioni, C. Scaling properties of seismicity and faulting. *Earth Planet. Sci. Lett.* **2022**, *584*, 117511. [[CrossRef](#)]
28. Varotsos, P.A.; Sarlis, N.V.; Tanaka, H.K.; Skordas, E.S. Similarity of fluctuations in correlated systems: The case of seismicity. *Phys. Rev. E* **2005**, *72*, 041103. [[CrossRef](#)]
29. Sarlis, N.V.; Skordas, E.S.; Varotsos, P.A. Similarity of fluctuations in systems exhibiting Self-Organized Criticality. *Europhys. Lett.* **2011**, *96*, 28006. [[CrossRef](#)]
30. Sarlis, N.V.; Skordas, E.S.; Varotsos, P.A. The change of the entropy in natural time under time-reversal in the Olami-Feder-Christensen earthquake model. *Tectonophysics* **2011**, *513*, 49–53. [[CrossRef](#)]
31. Sarlis, N.V.; Skordas, E.S.; Varotsos, P.A.; Ramírez-Rojas, A.; Flores-Márquez, E.L. Natural time analysis: On the deadly Mexico M8.2 earthquake on 7 September 2017. *Phys. A* **2018**, *506*, 625–634. [[CrossRef](#)]
32. Olami, Z.; Feder, H.J.S.; Christensen, K. Self-organized criticality in a continuous, nonconservative cellular automaton modeling earthquakes. *Phys. Rev. Lett.* **1992**, *68*, 1244–1247. [[CrossRef](#)]
33. Ramos, O.; Altshuler, E.; Måløy, K.J. Quasiperiodic Events in an Earthquake Model. *Phys. Rev. Lett.* **2006**, *96*, 098501. [[CrossRef](#)]
34. Caruso, F.; Kantz, H. Prediction of extreme events in the OFC model on a small world network. *Eur. Phys. J. B* **2011**, *79*, 7–11. [[CrossRef](#)]
35. Varotsos, P.A.; Sarlis, N.V.; Skordas, E.S.; Lazaridou, M.S. Identifying sudden cardiac death risk and specifying its occurrence time by analyzing electrocardiograms in natural time. *Appl. Phys. Lett.* **2007**, *91*, 064106. [[CrossRef](#)]
36. Varotsos, P.A.; Sarlis, N.V.; Skordas, E.S. Study of the temporal correlations in the magnitude time series before major earthquakes in Japan. *J. Geophys. Res. Space Phys.* **2014**, *119*, 9192–9206. [[CrossRef](#)]
37. Varotsos, P.A.; Sarlis, N.V.; Skordas, E.S.; Lazaridou, M.S. Seismic Electric Signals: An additional fact showing their physical interconnection with seismicity. *Tectonophysics* **2013**, *589*, 116–125. [[CrossRef](#)]
38. Varotsos, P.; Lazaridou, M. Latest aspects of earthquake prediction in Greece based on Seismic Electric Signals. *Tectonophysics* **1991**, *188*, 321–347. [[CrossRef](#)]
39. Sarlis, N.; Varotsos, P. Magnetic field near the outcrop of an almost horizontal conductive sheet. *J. Geodyn.* **2002**, *33*, 463–476. [[CrossRef](#)]

40. Varotsos, P.A.; Sarlis, N.V.; Skordas, E.S. Electric Fields that “arrive” before the time derivative of the magnetic field prior to major earthquakes. *Phys. Rev. Lett.* **2003**, *91*, 148501. [[CrossRef](#)]
41. Skordas, E.; Sarlis, N. On the anomalous changes of seismicity and geomagnetic field prior to the 2011 9.0 Tohoku earthquake. *J. Asian Earth Sci.* **2014**, *80*, 161–164. [[CrossRef](#)]
42. Varotsos, P.A.; Sarlis, N.V.; Skordas, E.S.; Uyeda, S.; Kamogawa, M. Natural time analysis of critical phenomena. *Proc. Natl. Acad. Sci. USA* **2011**, *108*, 11361–11364. [[CrossRef](#)]
43. Sarlis, N.V.; Skordas, E.S.; Lazaridou, M.S.; Varotsos, P.A. Investigation of seismicity after the initiation of a Seismic Electric Signal activity until the main shock. *Proc. Jpn. Acad. Ser. B Phys. Biol. Sci.* **2008**, *84*, 331–343. [[CrossRef](#)]
44. Vallianatos, F.; Michas, G.; Benson, P.; Sammonds, P. Natural time analysis of critical phenomena: The case of acoustic emissions in triaxially deformed Etna basalt. *Phys. A* **2013**, *392*, 5172–5178. [[CrossRef](#)]
45. Sarlis, N.V.; Christopoulos, S.R.G.; Bemplidaki, M.M. Change  $\Delta S$  of the entropy in natural time under time reversal: Complexity measures upon change of scale. *Europhys. Lett.* **2015**, *109*, 18002. [[CrossRef](#)]
46. Pasari, S. Nowcasting Earthquakes in the Bay of Bengal Region. *Pure Appl. Geophys.* **2019**, *176*, 1417–1432. [[CrossRef](#)]
47. Baldoumas, G.; Peschos, D.; Tatsis, G.; Chronopoulos, S.K.; Christofilakis, V.; Kostarakis, P.; Varotsos, P.; Varotsos, N.V.; Skordas, E.S.; Bechlioulis, A.; et al. A Prototype Photoplethysmography Electronic Device that Distinguishes Congestive Heart Failure from Healthy Individuals by Applying Natural Time Analysis. *Electronics* **2019**, *8*, 1288. [[CrossRef](#)]
48. Varotsos, P.A.; Sarlis, N.V.; Skordas, E.S. Phenomena preceding major earthquakes interconnected through a physical model. *Ann. Geophys.* **2019**, *37*, 315–324. [[CrossRef](#)]
49. Pasari, S.; Verma, H.; Sharma, Y.; Choudhary, N. Spatial distribution of seismic cycle progression in northeast India and Bangladesh regions inferred from natural time analysis. *Acta Geophys.* **2023**, *71*, 89–100. [[CrossRef](#)]
50. Varotsos, C.A.; Tzani, C. A new tool for the study of the ozone hole dynamics over Antarctica. *Atmos. Environ.* **2012**, *47*, 428–434. [[CrossRef](#)]
51. Varotsos, C.A.; Tzani, C.; Cracknell, A.P. Precursory signals of the major El Niño Southern Oscillation events. *Theor. Appl. Climatol.* **2016**, *124*, 903–912. [[CrossRef](#)]
52. Mintzelas, A.; Sarlis, N. Minima of the fluctuations of the order parameter of seismicity and earthquake networks based on similar activity patterns. *Phys. A* **2019**, *527*, 121293. [[CrossRef](#)]
53. Pasari, S.; Sharma, Y. Contemporary Earthquake Hazards in the West-Northwest Himalaya: A Statistical Perspective through Natural Times. *Seismol. Res. Lett.* **2020**, *91*, 3358–3369. [[CrossRef](#)]
54. Pasari, S.; Simanjuntak, A.V.H.; Mehta, A.; Neha.; Sharma, Y. The Current State of Earthquake Potential on Java Island, Indonesia. *Pure Appl. Geophys.* **2021**, *178*, 2789–2806. [[CrossRef](#)]
55. Pasari, S.; Simanjuntak, A.V.H.; Neha.; Sharma, Y. Nowcasting earthquakes in Sulawesi Island, Indonesia. *Geosci. Lett.* **2021**, *8*, 27. [[CrossRef](#)]
56. Pasari, S.; Simanjuntak, A.V.H.; Mehta, A.; Neha.; Sharma, Y. A synoptic view of the natural time distribution and contemporary earthquake hazards in Sumatra, Indonesia. *Nat. Hazards* **2021**, *108*, 309–321. [[CrossRef](#)]
57. Brillinger, D.R. Time series, point processes, and hybrids. *Can. J. Stat.* **1994**, *22*, 177–206. [[CrossRef](#)]
58. Hanks, T.C.; Kanamori, H. A moment magnitude scale. *J. Geophys. Res.* **1979**, *84*, 2348–2350. [[CrossRef](#)]
59. Skordas, E.S.; Christopoulos, S.R.G.; Sarlis, N.V. Detrended fluctuation analysis of seismicity and order parameter fluctuations before the M7.1 Ridgecrest earthquake. *Nat. Hazards* **2020**, *100*, 697–711. [[CrossRef](#)]
60. Sarlis, N.V.; Skordas, E.S.; Varotsos, P.A.; Ramírez-Rojas, A.; Flores-Márquez, E.L. Identifying the Occurrence Time of the Deadly Mexico M8.2 Earthquake on 7 September 2017. *Entropy* **2019**, *21*, 301. [[CrossRef](#)]
61. Christopoulos, S.R.G.; Varotsos, P.K.; Perez-Oregon, J.; Papadopoulou, K.A.; Skordas, E.S.; Sarlis, N.V. Natural Time Analysis of Global Seismicity. *Appl. Sci.* **2022**, *12*, 7496. [[CrossRef](#)]
62. Vallianatos, F.; Karakostas, V.; Papadimitriou, E. A Non-Extensive Statistical Physics View in the Spatiotemporal Properties of the 2003 (Mw6.2) Lefkada, Ionian Island Greece, Aftershock Sequence. *Pure Appl. Geophys.* **2014**, *171*, 1343–1354. [[CrossRef](#)]
63. Turcotte, D.L. *Fractals and Chaos in Geology and Geophysics*, 2nd ed.; Cambridge University Press: Cambridge, UK, 1997. [[CrossRef](#)]
64. Varotsos, P.A.; Sarlis, N.V.; Tanaka, H.K.; Skordas, E.S. Some properties of the entropy in the natural time. *Phys. Rev. E* **2005**, *71*, 032102. [[CrossRef](#)] [[PubMed](#)]
65. Lesche, B. Instabilities of Renyi entropies. *J. Stat. Phys.* **1982**, *27*, 419. [[CrossRef](#)]
66. Lesche, B. Renyi entropies and observables. *Phys. Rev. E* **2004**, *70*, 017102. [[CrossRef](#)] [[PubMed](#)]
67. Sarlis, N.V. Entropy in Natural Time and the Associated Complexity Measures. *Entropy* **2017**, *19*, 177. [[CrossRef](#)]
68. Sarlis, N.V.; Skordas, E.S.; Varotsos, P.A. A remarkable change of the entropy of seismicity in natural time under time reversal before the super-giant M9 Tohoku earthquake on 11 March 2011. *EPL (Europhys. Lett.)* **2018**, *124*, 29001. [[CrossRef](#)]
69. Ramírez-Rojas, A.; Flores-Márquez, E.L.; Sarlis, N.V.; Varotsos, P.A. The Complexity Measures Associated with the Fluctuations of the Entropy in Natural Time before the Deadly Mexico M8.2 Earthquake on 7 September 2017. *Entropy* **2018**, *20*, 477. [[CrossRef](#)]
70. Varotsos, P.A.; Sarlis, N.V.; Skordas, E.S. Identifying the occurrence time of an impending major earthquake: A review. *Earthq. Sci.* **2017**, *30*, 209–218. [[CrossRef](#)]

71. Potirakis, S.M.; Contoyiannis, Y.; Schekotov, A.; Eftaxias, K.; Hayakawa, M. Evidence of critical dynamics in various electromagnetic precursors. *Eur. Phys. J. Spec. Top.* **2021**, *230*, 151–177. [[CrossRef](#)]
72. Potirakis, S.M.; Karadimitrakis, A.; Eftaxias, K. Natural time analysis of critical phenomena: The case of pre-fracture electromagnetic emissions. *Chaos* **2013**, *23*, 023117. [[CrossRef](#)]
73. Potirakis, S.M.; Schekotov, A.; Contoyiannis, Y.; Balasis, G.; Koulouras, G.E.; Melis, N.S.; Boutsis, A.Z.; Hayakawa, M.; Eftaxias, K.; Nomicos, C. On Possible Electromagnetic Precursors to a Significant Earthquake (Mw = 6.3) Occurred in Lesvos (Greece) on 12 June 2017. *Entropy* **2019**, *21*, 241. [[CrossRef](#)]
74. Potirakis, S.M.; Eftaxias, K.; Schekotov, A.; Yamaguchi, H.; Hayakawa, M. Criticality features in ultra-low frequency magnetic fields prior to the 2013 M6.3 Kobe earthquake. *Ann. Geophys.* **2016**, *59*, S0317. [[CrossRef](#)]
75. Hayakawa, M.; Schekotov, A.; Potirakis, S.; Eftaxias, K. Criticality features in ULF magnetic fields prior to the 2011 Tohoku earthquake. *Proc. Jpn. Acad. Ser. B Phys. Biol. Sci.* **2015**, *91*, 25–30. [[CrossRef](#)] [[PubMed](#)]
76. Hayakawa, M.; Schekotov, A.; Potirakis, S.; Eftaxias, K.; Li, Q.; Asano, T. An Integrated Study of ULF Magnetic Field Variations in Association with the 2008 Sichuan Earthquake, on the Basis of Statistical and Critical Analyses. *Open J. Earthq. Res.* **2015**, *4*, 85–93. [[CrossRef](#)]
77. Potirakis, S.M.; Schekotov, A.; Asano, T.; Hayakawa, M. Natural time analysis on the ultra-low frequency magnetic field variations prior to the 2016 Kumamoto (Japan) earthquakes. *J. Asian Earth Sci.* **2018**, *154*, 419–427. [[CrossRef](#)]
78. Vallianatos, F.; Michas, G.; Hloupis, G.; Chatzopoulos, G. The Evolution of Preseismic Patterns Related to the Central Crete (Mw6.0) Strong Earthquake on 27 September 2021 Revealed by Multiresolution Wavelets and Natural Time Analysis. *Geosciences* **2022**, *12*, 33. [[CrossRef](#)]
79. Yang, S.S.; Potirakis, S.M.; Sasmal, S.; Hayakawa, M. Natural Time Analysis of Global Navigation Satellite System Surface Deformation: The Case of the 2016 Kumamoto Earthquakes. *Entropy* **2020**, *22*, 674. [[CrossRef](#)]
80. Sarlis, N.V.; Skordas, E.S.; Varotsos, P.A.; Nagao, T.; Kamogawa, M.; Tanaka, H.; Uyeda, S. Minimum of the order parameter fluctuations of seismicity before major earthquakes in Japan. *Proc. Natl. Acad. Sci. USA* **2013**, *110*, 13734–13738. [[CrossRef](#)]
81. Varotsos, P.; Alexopoulos, K. *Thermodynamics of Point Defects and Their Relation with Bulk Properties*; North Holland: Amsterdam, The Netherlands, 1986.
82. Uyeda, S.; Kamogawa, M.; Tanaka, H. Analysis of electrical activity and seismicity in the natural time domain for the volcanic-seismic swarm activity in 2000 in the Izu Island region, Japan. *J. Geophys. Res.* **2009**, *114*, B02310. [[CrossRef](#)]
83. Potirakis, S.M.; Contoyiannis, Y.; Melis, N.S.; Kopanas, J.; Antonopoulos, G.; Balasis, G.; Kontoes, C.; Nomicos, C.; Eftaxias, K. Recent seismic activity at Cephalonia (Greece): a study through candidate electromagnetic precursors in terms of non-linear dynamics. *Nonlin. Process. Geophys.* **2016**, *23*, 223–240. [[CrossRef](#)]
84. Flores-Márquez, E.L.; Ramírez-Rojas, A.; Perez-Oregon, J.; Sarlis, N.V.; Skordas, E.S.; Varotsos, P.A. Natural Time Analysis of Seismicity within the Mexican Flat Slab before the M7.1 Earthquake on 19 September 2017. *Entropy* **2020**, *22*, 730. [[CrossRef](#)]
85. Tsallis, C. *Introduction to Nonextensive Statistical Mechanics*; Springer: Berlin, Germany, 2009. [[CrossRef](#)]
86. Tsallis, C. Possible generalization of Boltzmann-Gibbs statistics. *J. Stat. Phys.* **1988**, *52*, 479–487. [[CrossRef](#)]
87. Sotolongo-Costa, O.; Posadas, A. Fragment-Asperity Interaction Model for Earthquakes. *Phys. Rev. Lett.* **2004**, *92*, 048501. [[CrossRef](#)] [[PubMed](#)]
88. Silva, R.; França, G.S.; Vilar, C.S.; Alcaniz, J.S. Nonextensive models for earthquakes. *Phys. Rev. E* **2006**, *73*, 026102. [[CrossRef](#)]
89. Tsallis, C. The Nonadditive Entropy Sq and Its Applications in Physics and Elsewhere: Some Remarks. *Entropy* **2011**, *13*, 1765–1804. [[CrossRef](#)]
90. Tsallis, C. Enthusiasm and Skepticism: Two Pillars of Science—A Nonextensive Statistics Case. *Physics* **2022**, *4*, 609–632. [[CrossRef](#)]
91. Posadas, A.; Sotolongo-Costa, O. Non-extensive entropy and fragment–asperity interaction model for earthquakes. *Commun. Nonlinear Sci. Numer. Simul.* **2023**, *117*, 106906. [[CrossRef](#)]
92. Lifshitz, I.; Slyozov, V. The kinetics of precipitation from supersaturated solid solutions. *J. Phys. Chem. Solids* **1961**, *19*, 35–50. [[CrossRef](#)]
93. Wagner, C. Theorie der Alterung von Niederschlägen durch Umlösen (Ostwald-Reifung). *Z. Für Elektrochem. Berichte Der Bunsenges. Für Phys. Chem.* **1961**, *65*, 581–591. [[CrossRef](#)]
94. Christopoulos, S.R.G.; Sarlis, N.V. An Application of the Coherent Noise Model for the Prediction of Aftershock Magnitude Time Series. *Complexity* **2017**, *2017*, 6853892. [[CrossRef](#)]
95. Hauksson, E.; Yang, W.; Shearer, P.M. Waveform Relocated Earthquake Catalog for Southern California (1981 to June 2011). *Bull. Seismol. Soc. Am.* **2012**, *102*, 2239–2244. [[CrossRef](#)]
96. Peng, C.K.; Buldyrev, S.V.; Havlin, S.; Simons, M.; Stanley, H.E.; Goldberger, A.L. Mosaic organization of DNA nucleotides. *Phys. Rev. E* **1994**, *49*, 1685–1689. [[CrossRef](#)] [[PubMed](#)]
97. Skordas, E.S.; Sarlis, N.V.; Varotsos, P.A. Precursory variations of Tsallis non-extensive statistical mechanics entropic index associated with the M9 Tohoku earthquake in 2011. *Eur. Phys. J. Spec. Top.* **2020**, *229*, 851–859. [[CrossRef](#)]
98. Varotsos, P.A.; Sarlis, N.V.; Skordas, E.S. Tsallis Entropy Index q and the Complexity Measure of Seismicity in Natural Time under Time Reversal before the M9 Tohoku Earthquake in 2011. *Entropy* **2018**, *20*, 757. [[CrossRef](#)]

99. Riquelme-Galván, M.; Robledo, A. Dual characterization of critical fluctuations: Density functional theory & nonlinear dynamics close to a tangent bifurcation. *Eur. Phys. J. Spec. Top.* **2017**, *226*, 433–442. [[CrossRef](#)]
100. Tsallis, C.; Gell-Mann, M.; Sato, Y. Extensivity and entropy production. *Europhys. News* **2005**, *36*, 186–189. [[CrossRef](#)]
101. Robledo, A. Critical fluctuations, intermittent dynamics and Tsallis statistics. *Phys. A* **2004**, *344*, 631–636. [[CrossRef](#)]
102. Robledo, A. Unorthodox properties of critical clusters. *Mol. Phys.* **2005**, *103*, 3025–3030. [[CrossRef](#)]
103. Abe, S. Stability of Tsallis entropy and instabilities of Rényi and normalized Tsallis entropies: A basis for q-exponential distributions. *Phys. Rev. E* **2002**, *66*, 046134. [[CrossRef](#)]

**Disclaimer/Publisher's Note:** The statements, opinions and data contained in all publications are solely those of the individual author(s) and contributor(s) and not of MDPI and/or the editor(s). MDPI and/or the editor(s) disclaim responsibility for any injury to people or property resulting from any ideas, methods, instructions or products referred to in the content.